JACS
JOURNAL OF THE AMERICAN CHEMICAL SOCIETY
pubs.acs.org/JACS
Article

An Asymmetric S_N2 Dynamic Kinetic Resolution

Nomaan M. Rezayee, Valdemar J. Enemærke, Sif T. Linde, Johannes N. Lamhauge, Gabriel J. Reyes-Rodríguez, Karl Anker Jørgensen,* Chenxi Lu, and K. N. Houk*

Cite This: J. Am. Chem. Soc. 2021, 143, 7509−7520
Read Online

ABSTRACT: The S_N2 reaction exhibits the classic Walden inversion, indicative of the stereospecific backside attack of the nucleophile on the stereogenic center. Observation of the inversion of the stereocenter provides evidence for an S_N2-type displacement. However, this maxim is contingent on substitution proceeding on a discrete stereocenter. Here we report an S_N2 reaction that leads to enantioenrichment of product despite starting from a racemic mixture of starting material. The enantioconvergent reaction proceeds through a dynamic Walden cycle, involving an equilibrating mixture of enantiomers, initiated by a chiral aminocatalyst and terminated by a stereoselective S_N2 reaction at a tertiary carbon to provide a quaternary carbon stereocenter. A combination of computational, kinetic, and empirical studies elucidates the multifaceted role of the chiral organocatalyst to provide a model example of the Curtin−Hammett principle. These examples challenge the notion of enantioenriched products exclusively arising from predefined stereocenters when operating through an S_N2 mechanism. Based on these principles, examples are included to highlight the generality of the mechanism. We anticipate the asymmetric S_N2 dynamic kinetic resolution to be used for a variety of future reactions.

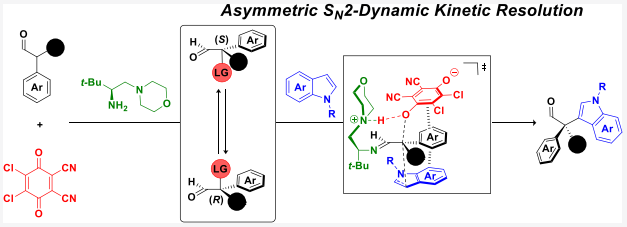

INTRODUCTION

The bimolecular nucleophilic substitution reaction (S_N2) is a fundamental mechanism in organic chemistry.[1] A key attribute of the S_N2 mechanism is the stereospecific "backside" attack of the nucleophile to the reactive carbon center, leading to the synchronous bond formation of the nucleophile with the bond cleavage of the leaving group as the rate-determining step, Scheme 1A.[2−4] The concerted substitution leads to the iconic Walden inversion, resulting in an absolute configuration opposite that of the starting material.[1,5] By this approach, the preparation of enantioenriched compounds necessitates substitution on a discrete, predefined stereocenter (Scheme 1B).

S_N2 substrates provide an appealing manifold for fundamental synthetic diversifications, which allows for the compilation of libraries with an array of nucleophiles and stereocenters. An attractive feature of these processes is the potential access to both absolute configurations through iterative stereospecific substitutions. This was first realized by Walden in 1896,[2] in what is known as the Walden cycle, for the stepwise conversion of (+)-malic acid to (−)-malic acid and back again (Scheme 1C).[6] Elements and principles of the Walden cycle have had a profound impact on the field of organic chemistry and has manifested into several powerful synthetic methodologies such as the Appel, Finkelstein, and Mitsunobu reactions,[7] etc. However, only a few dynamic versions of this Walden cycle—a dynamic interconversion of enantiomers of the substrate through an S_N2 substitution followed by a stereoselective S_N2 reaction (asymmetric S_N2 dynamic kinetic resolution)—have been reported.[8]

While an S_N2 mechanism is classically not stereodetermining (the latter is simply a function of the starting material stereochemistry), the stereospecificity of the reaction has been leveraged to access diastereoselective reactions.[9−12] However, due to the crowded, highly ordered transition state, the substitution is sensitive to steric hindrance and is generally limited to secondary stereocenters.[7] Despite this limitation, rare examples have been reported to furnish tetrasubstituted tertiary stereocenters.[13−18] Nevertheless, stereoselective examples remain contingent on the enantiopurity of the starting material bearing the leaving group (Scheme 1B).

Several stereoselective strategies have been developed to install leaving groups in an enantioconvergent manner. Among these approaches, dynamic kinetic resolution (DKR) pathways have distinguished themselves as an operationally facile and efficient approach to provide compounds with high enantioselectivity.[8,19−25] DKR processes hinge on two distinct catalytic cycles. The first involves the rapid interconversion of one stereocenter of a compound to another (stereomutative transformation). The second slower cycle proceeds to

Received: March 4, 2021
Published: May 4, 2021

https://doi.org/10.1021/jacs.1c02193
J. Am. Chem. Soc. 2021, 143, 7509−7520

Scheme 1. (A) S_N2 Mechanism Depicting the Stereospecific Substitution; (B) Typical Results from an S_N2 Reaction; Rare Example of Enantioenrichment from an S_N2 Reaction (This Work, Gray); (C) The Classical Walden Cycle

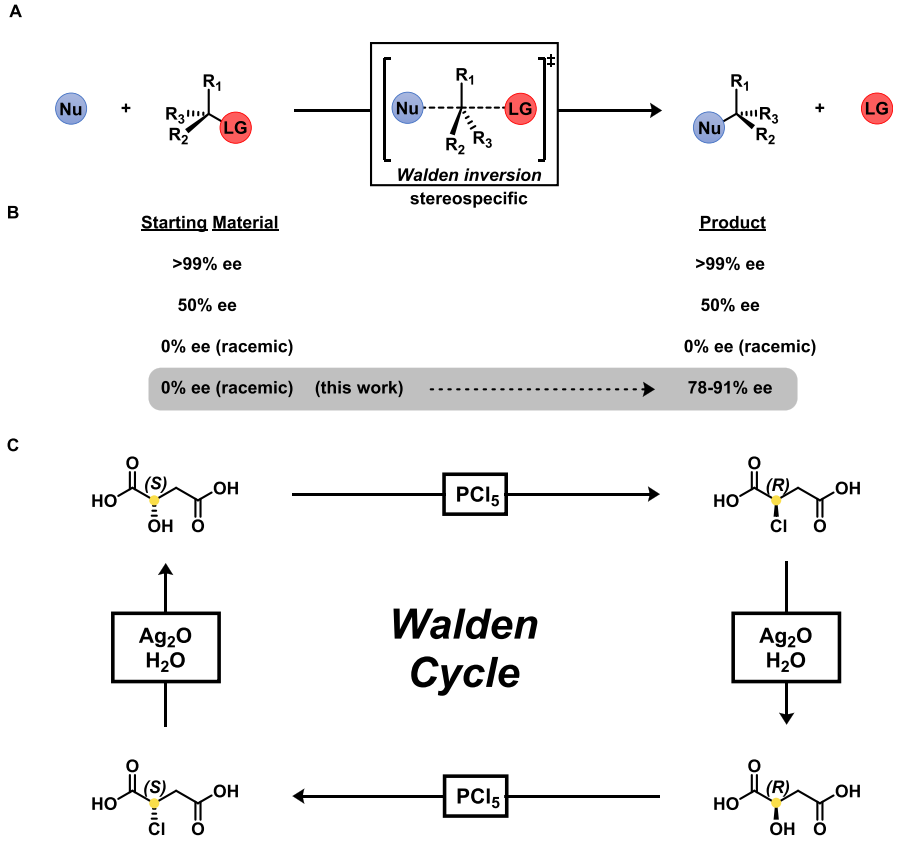

Scheme 2. (A) Aminocatalytic Oxidative Coupling of α-Branched Aldehydes 1 with Indoles 2; (B) Possible Reaction Courses

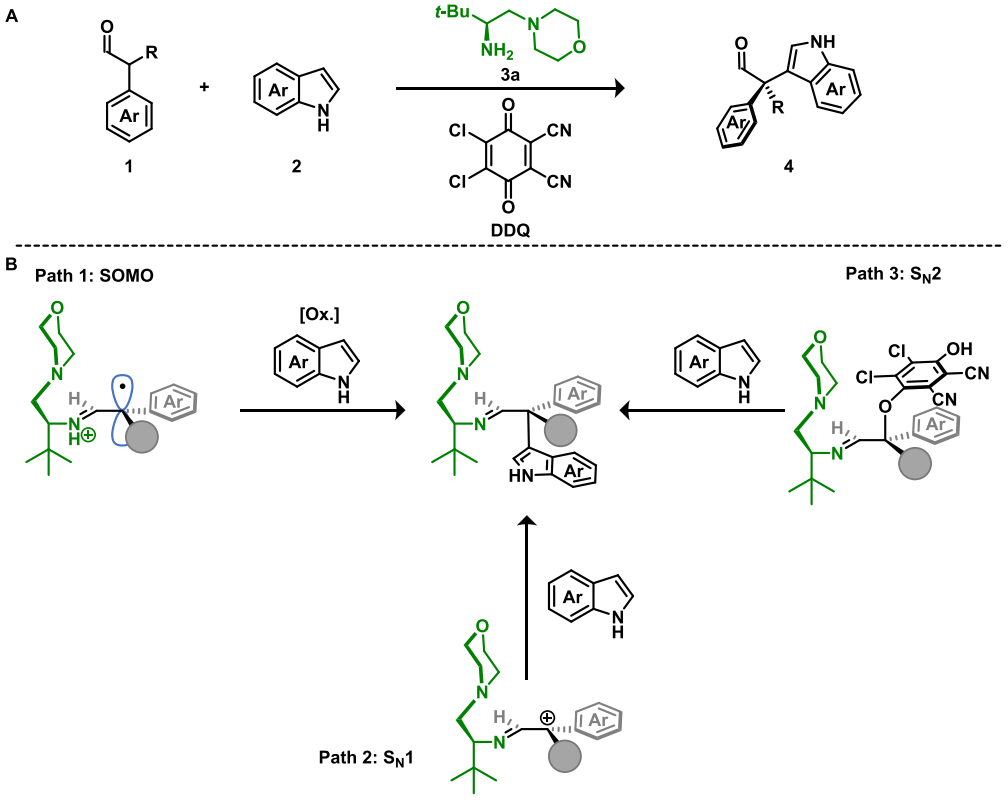

https://doi.org/10.1021/jacs.1c02193
J. Am. Chem. Soc. 2021, 143, 7509−7520

Scheme 3. (A) The Two Different Oxidation Pathways Investigated Computationally: Radical Generation *vs* Two-Electron Oxidation; (B) Calculated Energy Profiles for the Two Different Oxidation Pathways

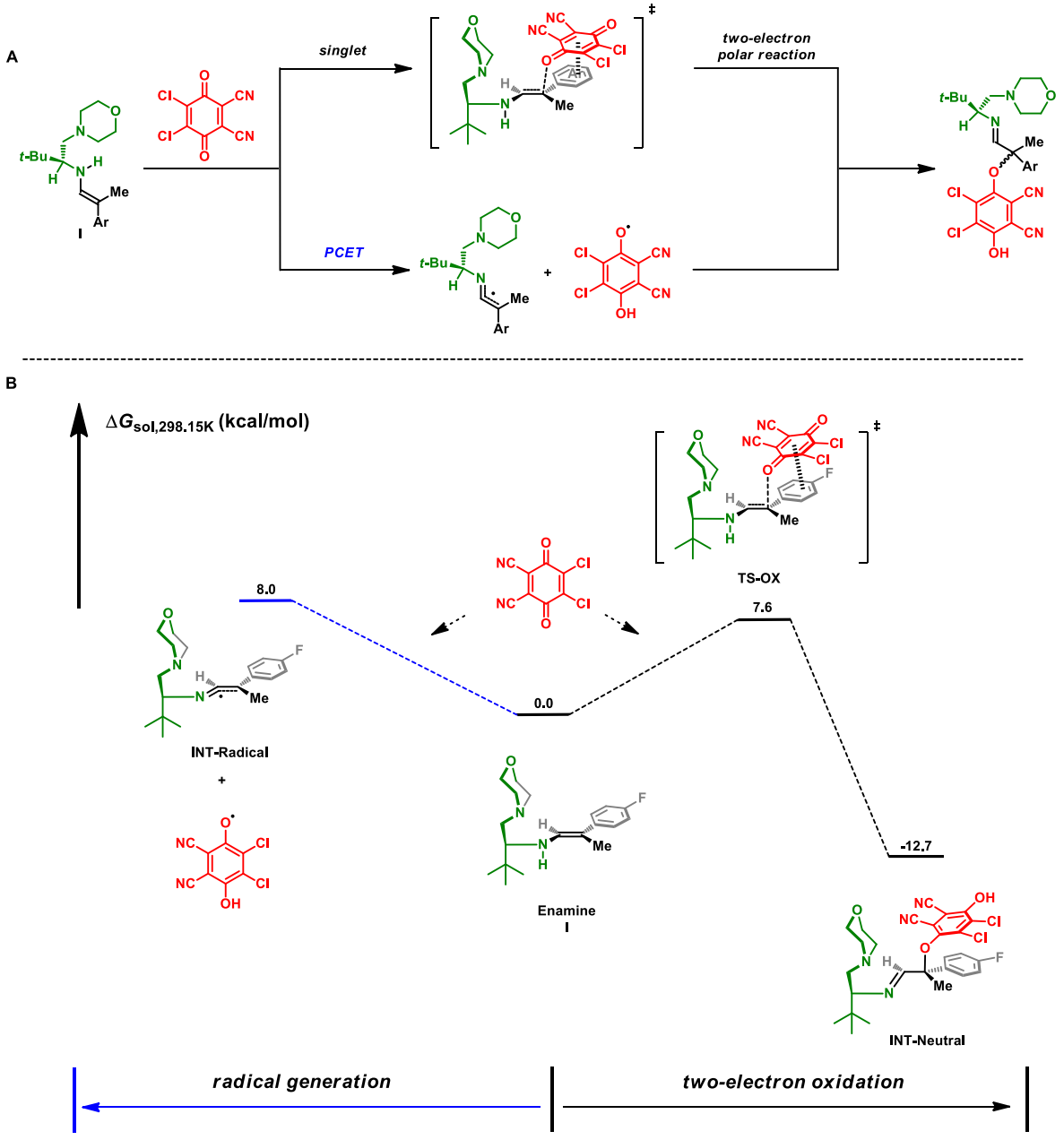

selectively and irreversibly convert one enantiomer to product. In marked contrast to kinetic resolution processes, DKR pathways provide theoretical yields and enantioselectivity of up to 100%.[26,27]

Here we present an asymmetric S_N2 dynamic kinetic resolution (S_N2-DKR) mechanism leading to the formation of enantiomerically enriched stereocenters. In stark contrast to previous methods,[18] the reaction proceeds via an unselective, amino-catalyzed installation of an *O*-bound quinol leaving group. Combined computational and experimental investigations support an unprecedented amino-catalyzed S_N2-DKR event promoted by the endogenous leaving group, prior to an irreversible S_N2, to stereoselectively forge a C−C bond. Mechanistic studies elucidate a unique trifunctional role of the aminocatalyst: (1) HOMO-raising by enamine formation prior to oxidation, (2) stereomutative transformation via directed leaving group installation, and (3) kinetic resolution through activation of the leaving group. Despite the stereospecificity of the S_N2 reaction, the stereomutative transformation preceding the rate-determining substitution renders the S_N2 step as stereodetermining.

RESULTS AND DISCUSSION

Stereoselective construction of quaternary carbon centers (substituted by four carbons) is a long-standing challenge in organic chemistry.[28,29] We have been pursuing the development of novel methodologies to construct tetrasubstituted tertiary centers based on an amino-catalyzed oxidative coupling strategy wherein α-branched aldehydes are coupled to a variety of nucleophiles at a tertiary site.[18,30−32] The amino acid derived primary amine catalyst **3a**, bearing a pendent tertiary amine, proved critical for satisfactory stereoselectivity. Notably,

https://doi.org/10.1021/jacs.1c02193
J. Am. Chem. Soc. 2021, 143, 7509−7520

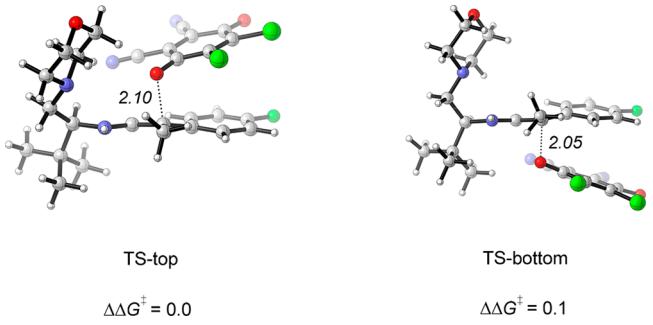

Figure 1. Transition state structures for the two possible approaches of DDQ to the enamine intermediate **I** and the free energy differences calculated at the (SMD:CH_2Cl_2)-ωB97X-D/def2-TZVPP//(SMD:CH_2Cl_2)-ωB97X-D/6-311G(d,p) level of theory. Energies are denoted in kcal/mol. Bond lengths are denoted in Å.

previous studies of related reactions have suggested an enantioselective oxidation preceding an S_N2 substitution.[18] During the course of our studies, indole **2** was identified as a suitable carbon-based nucleophile for the stereoselective construction of quaternary carbon centers with only electron-rich arenes (Scheme 2A).[31] Further attempts to develop a general methodology proved unfruitful. Due to the synthetic challenge of forming quaternary carbon stereocenters in an enantioselective manner,[33] we pursued mechanistic studies to improve the understanding of the reaction pathway in hopes of discovering a more general methodology.

There are at least three plausible pathways for the transformation shown in Scheme 2A. Path 1, employing singly occupied molecular orbital (SOMO)-activation, enlists a nascent radical formed upon single-electron oxidation, which combines with the carbon-based nucleophile and is subsequently oxidized a second time.[34,35] The second pathway (path 2) invokes a similar covalent activation strategy, but proceeds through a two-electron oxidation to form a cationic intermediate prior to nucleophile addition (S_N1).[36] Finally, path 3 operates through an inner-sphere two-electron oxidation by the quinone oxidant, effectively installing a leaving group that is displaced upon attack from the incoming nucleophile (S_N2).

Formation and isolation of the neutral *O*-bound 2,3-dichloro-5,6-dicyano-1,4-benzoquinone (DDQ) adduct (Scheme 2B, path 3) provided unambiguous evidence of a two-electron oxidation preceding nucleophilic addition, which excludes path 1 as the predominant pathway.[18] Furthermore, unlike previously reported quinol adducts, these proved to be remarkably labile leaving groups toward substitution; however, it remained unclear whether the DDQ adduct acted as a cationic reservoir or if it was displaced in a nucleophilic attack.

Oxidation and Installation of a Leaving Group. Previous studies by Mayr[37] and List,[38] employing related carbonyl compounds with quinones, yielded contrasting conclusions on the mechanism of oxidation. Mayr et al. provided evidence for a two-electron polar mechanism, while List et al. deduced that the reaction occurred by a proton-coupled electron transfer (PCET) pathway. Notably, different activation strategies and quinones were used, leaving the mechanism of oxidation ambiguous with aminocatalyst **3a**. While rate studies typically aid in the differentiation of various pathways, due to the heterogeneity of the oxidation step, we utilized computational studies to further investigate the oxidation event and to distinguish potential pathways for the complete umpolung coupling.

The two different oxidation paths outlined in Scheme 3A were evaluated. First, the α-branched aldehyde couples with the primary amine catalyst to generate an enamine intermediate **I**. From this intermediate the top reaction pathway involves a nucleophilic attack of the enamine carbon on the electrophilic oxygen atom in DDQ through a two-electron polar reaction path in a singlet state. The bottom reaction path describes a PCET pathway proceeding via an

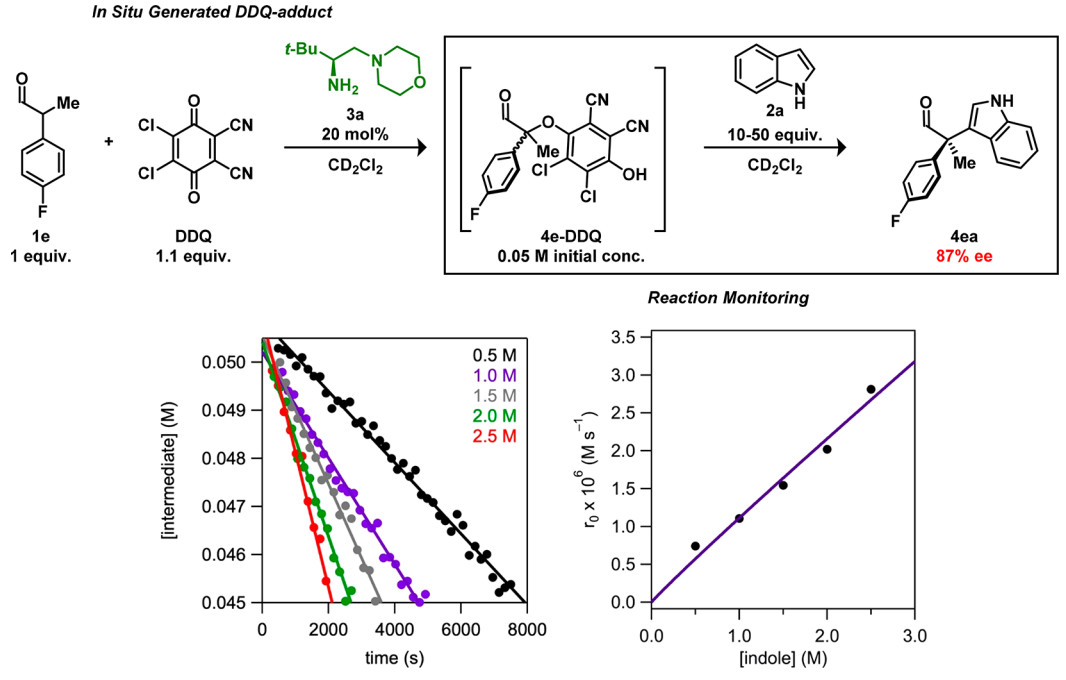

Figure 2. Top: Reaction investigated kinetically. Bottom-left: Concentration of intermediate **4e-DDQ** as a function of time for different indole **2a** concentrations. Bottom-right: Initial reaction rate as a function of indole **2a** concentration.

https://doi.org/10.1021/jacs.1c02193
J. Am. Chem. Soc. 2021, 143, 7509−7520

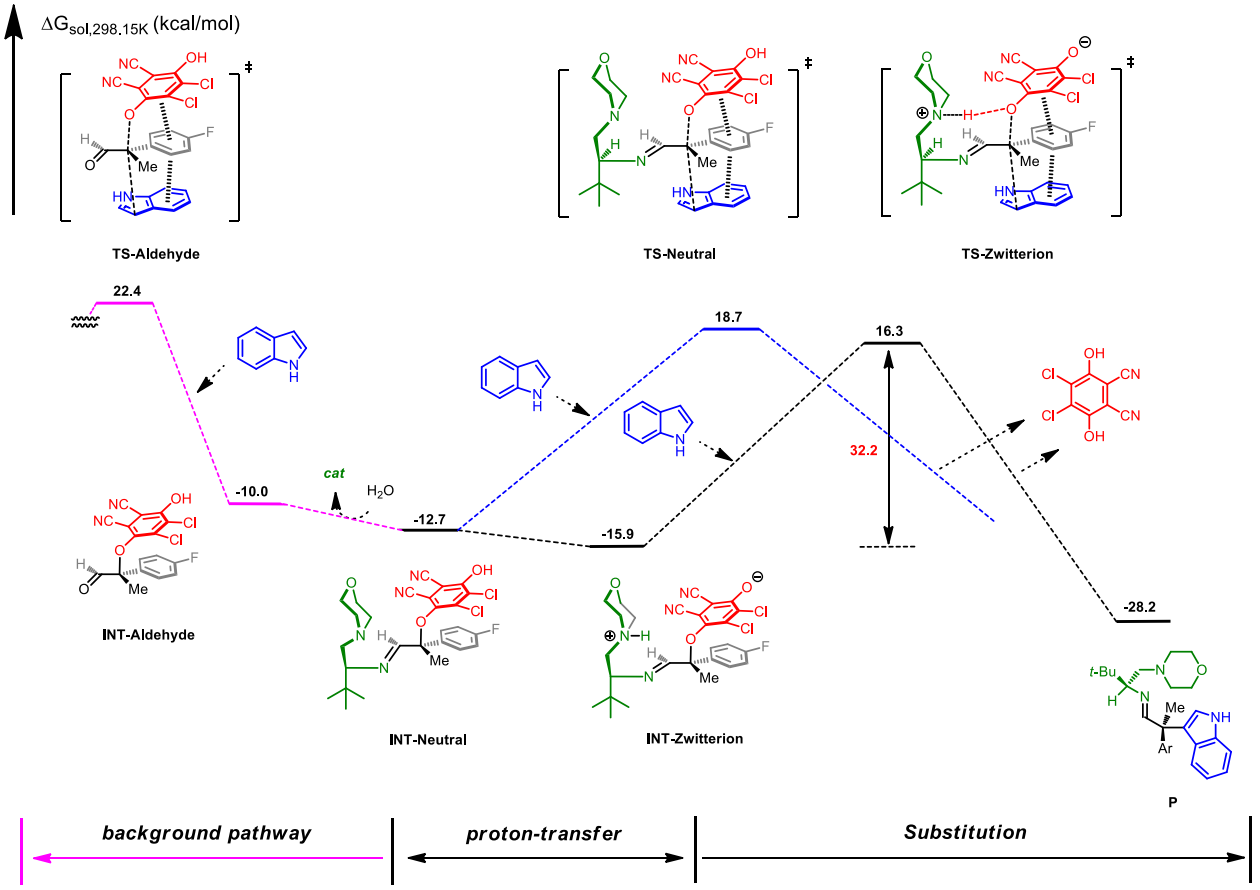

Figure 3. Calculated energy profile for the S_N2 reaction to the right and the uncatalyzed S_N2 background reaction to the left at the (SMD:CH_2Cl_2)-ωB97X-D/def2-TZVPP//(SMD:CH_2Cl_2)-M06-2X/6-31G(d) level of theory. Energies are denoted in kcal/mol.

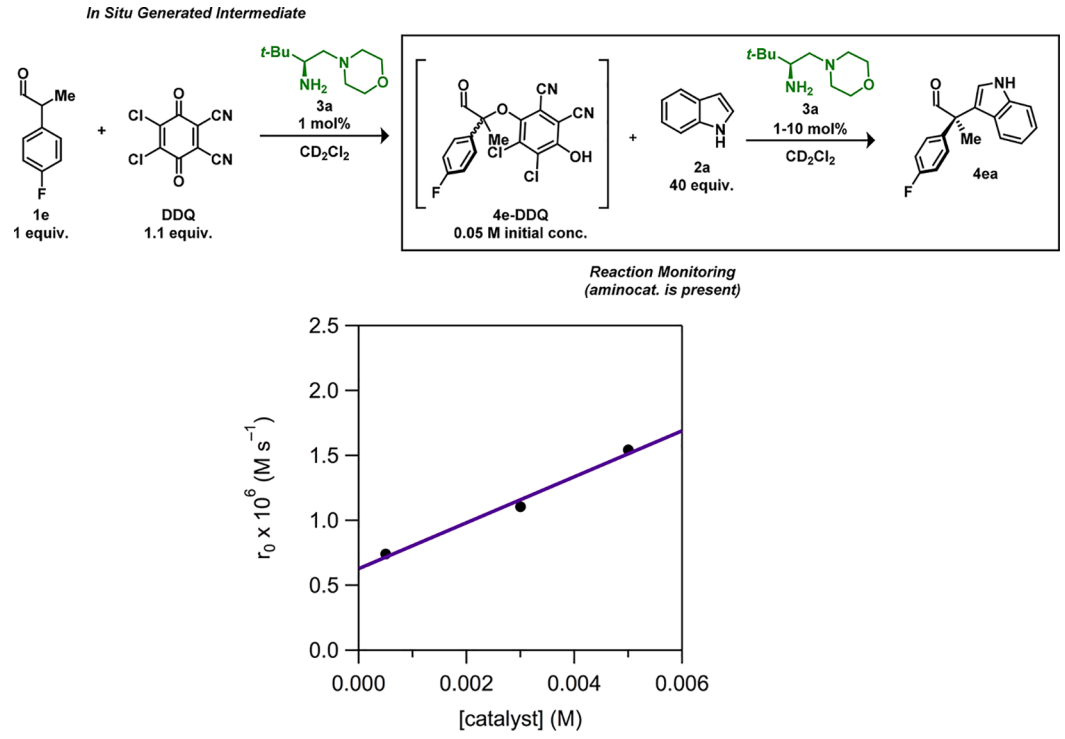

Figure 4. Top: Reaction investigated kinetically. Bottom: Initial reaction rate as a function of organocatalyst concentration.

outer-sphere single-electron oxidation and proton transfer to generate a radical pair, which then recombines.

These two pathways were computationally explored and are summarized in Scheme 3B. The formation of the enamine

https://doi.org/10.1021/jacs.1c02193
J. Am. Chem. Soc. 2021, 143, 7509−7520

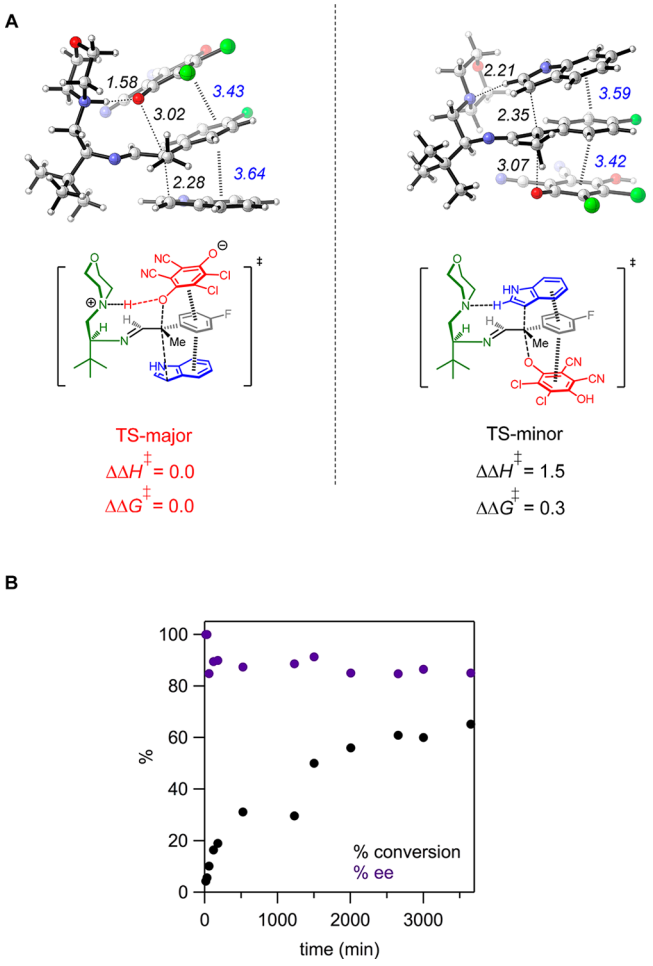

Figure 5. (A) Transition state structures for the two possible S_N2 reactions calculated at the (SMD:CH_2Cl_2)-ωB97X-D/def2-TZVPP//(SMD:CH_2Cl_2)-ωB97X-D/6-311G(d,p) level of theory. Truhlar's quasi-harmonic corrections were applied for $\Delta\Delta G^{\ddagger}$ with the frequency cutoff of 100 cm^{-1}. (B) Enantiomeric excess as a function of time. Energies are denoted in kcal/mol. Bond lengths are denoted in Å.

intermediate **I** is exergonic by 1.6 kcal/mol. Evaluation of the radical pathway provided an uphill free energy change for the PCET pathway of 8.0 kcal/mol. The thermodynamic feasibility suggests that this radical pair may be present and/or involved in the reaction. Alternatively, the direct two-electron inner-sphere oxidation of the enamine with DDQ proceeds with only a 7.6 kcal/mol energy barrier to yield the DDQ adduct. The subsequent proton transfer from nitrogen to oxygen is presumed to be mediated by a weak base (amine) and acid (water) present in the reaction mixture.

The computational study indicated that the two-electron oxidation (top reaction path, Scheme 3A) is the predominant pathway, but only marginally. With the feasibility of both pathways determined, we aimed to experimentally interrogate the oxidation event. A radical clock experiment, employing an α-branched aldehyde bearing a cyclopropyl group (**1f**), was performed in order to probe for a radical pair species, shown in eq 1. Under these conditions, the two-electron-oxidized intermediate **4l-DDQ** was formed in combination with the ring-opened diene **5** in a 3:1 ratio. While the DDQ adduct **4l-DDQ** with the radical clock intact was the major product, the ring-opened diene **5** provides indirect evidence of a fleeting radical species.

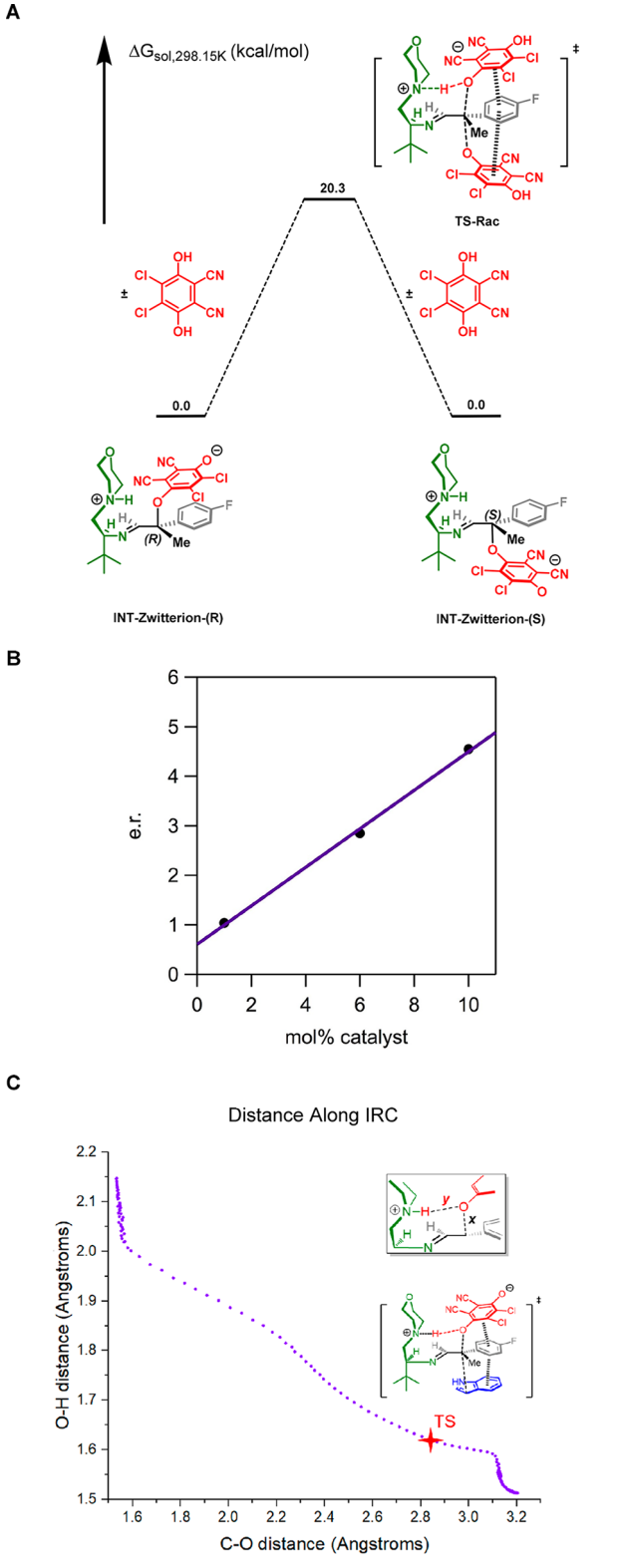

Figure 6. (A) Calculated energy profile for the (*R*)-zwitterionic intermediate in equilibrium with its (*S*)-diastereomer at the (SMD:CH_2Cl_2)-ωB97X-D/def2-TZVPP//(SMD:CH_2Cl_2)-M06-2X/6-31G(d) level of theory. (B) Enantiomeric excess as a function of organocatalyst loadings. (C) Intrinsic reaction coordinate calculation for the S_N2 process at the (SMD:CH_2Cl_2)-M06-2X/6-31G(d) level of theory. Energies are denoted in kcal/mol.

https://doi.org/10.1021/jacs.1c02193
J. Am. Chem. Soc. 2021, 143, 7509−7520

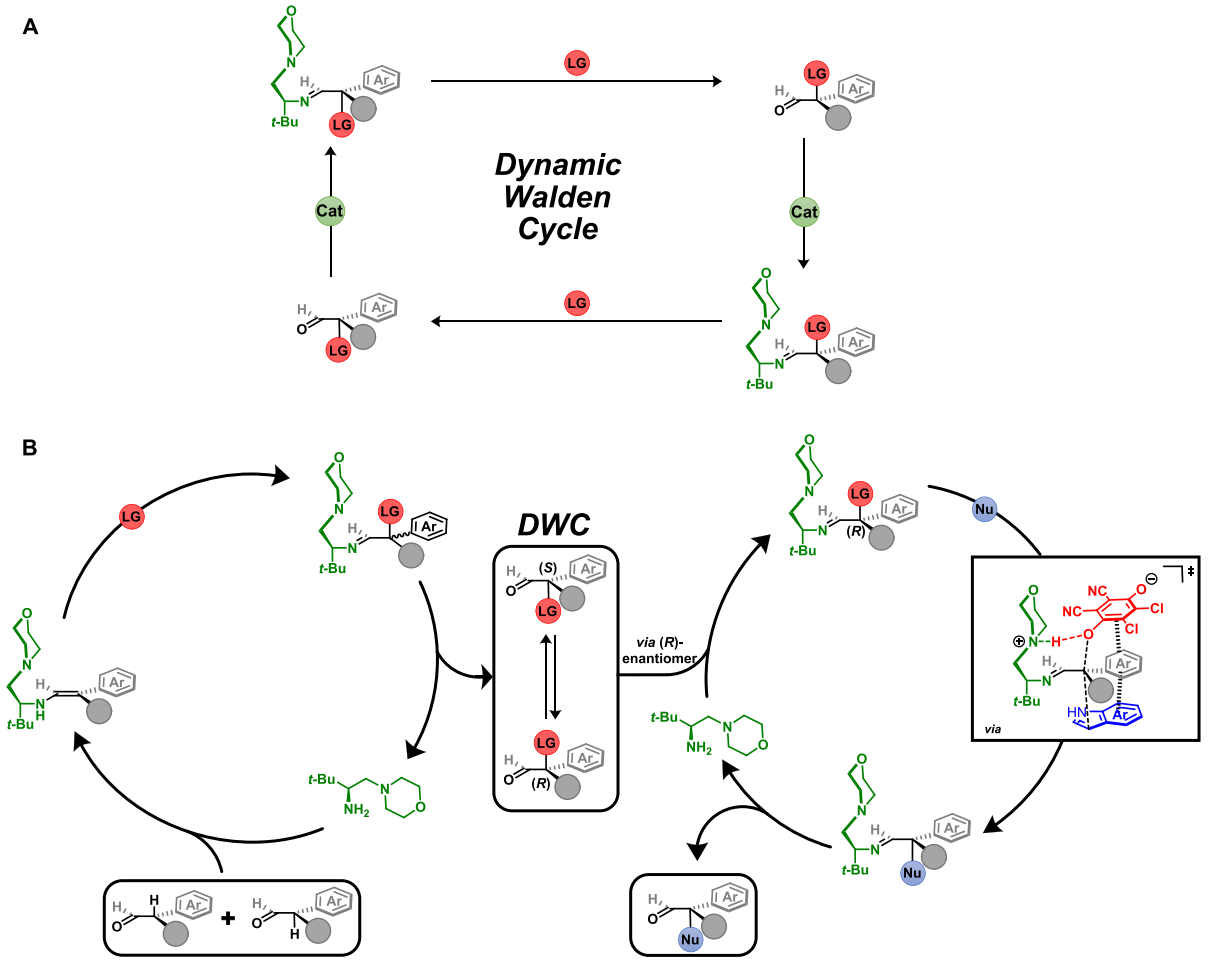

Figure 7. (A) Racemization via amino-catalyzed dynamic Walden cycle (DWC). (B) Trifunctional role of the aminocatalyst: (left) oxidation via enamine catalysis; (center) amino-catalyzed DWC; (right) activation of the leaving group for termination of the dynamic kinetic resolution by S_N2 substitution.

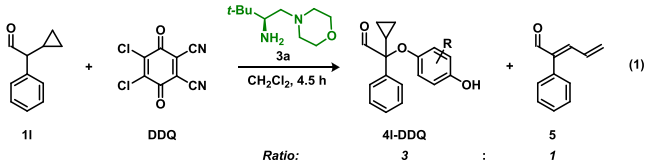

In the two-electron polar reaction path (Scheme 3A, top), DDQ approaches the enamine intermediate **I** from the same site as the morpholine moiety of the primary amine catalyst. Further evaluation of the direct attack of DDQ on **I**, for the "two-electron oxidation" pathway leads to an unexpected feature. In stark contrast to other methodologies, the installation of the leaving group in this case is stereochemically unselective, as the energy difference is only 0.1 kcal/mol for the diastereomeric transition states (Figure 1). The incoming DDQ fails to distinguish between the morpholine and the *tert*-butyl moieties.

Formation of an All-Carbon Quaternary Stereocenter. With the pathway of the installation of the leaving group identified, we set out to gain insight into this atypical substitution. We undertook rate studies to probe the kinetic order of the reaction postoxidation. The DDQ adduct was generated *in situ*, and the reaction was monitored (Figure 2, top; see Supporting Information). Under these conditions (pseudo-first-order), the reaction of this adduct with indole proceeded cleanly with first-order kinetic behavior attributed to first-order dependence of the DDQ adduct. Subsequent rate studies perturbing the concentration of indole lead to proportional deviation in r_o shown in Figure 2, bottom. Plotting the initial rate of the reaction as a function of indole concentration gave a linear relationship, also illustrating a first-order dependence in indole.[39] Taken together, these data are consistent with an S_N2 mechanism (Scheme 2B, path 3). Despite the changes in nucleophile concentration, in all cases 87% ee was obtained. Notably, the intersection through the origin in Figure 2, bottom, suggests no S_N1 character, eliminating path 2 in Scheme 2B as a major contributor to the overall reaction mechanism.

We computationally explored the nature of the reactive species and possible pathways for this step (Figure 3). The free energy profiles calculated for these three substitution pathways are shown in Figure 3. Beginning with the two imine intermediates, the equilibrium favors the zwitterionic species by 3.2 kcal/mol. Notably, a "triple π-stacking" among the attacking indole, the aryl substituent of the imine, and the hydroquinone leaving group is observed in all substitution transition states. An S_N2 reaction at a tertiary center is impeded due to its highly substituted nature and is calculated to be the rate-determining step in this case. The transition state originating from the zwitterionic species has an extra hydrogen bond between the morpholine moiety and the leaving

https://doi.org/10.1021/jacs.1c02193
J. Am. Chem. Soc. 2021, 143, 7509−7520

Scheme 4. Application of S_N2-DKR for the General Organocatalytic Oxidative Coupling of α-Branched Aldehydes with Indoles for the Formation of Quaternary Carbon[a]

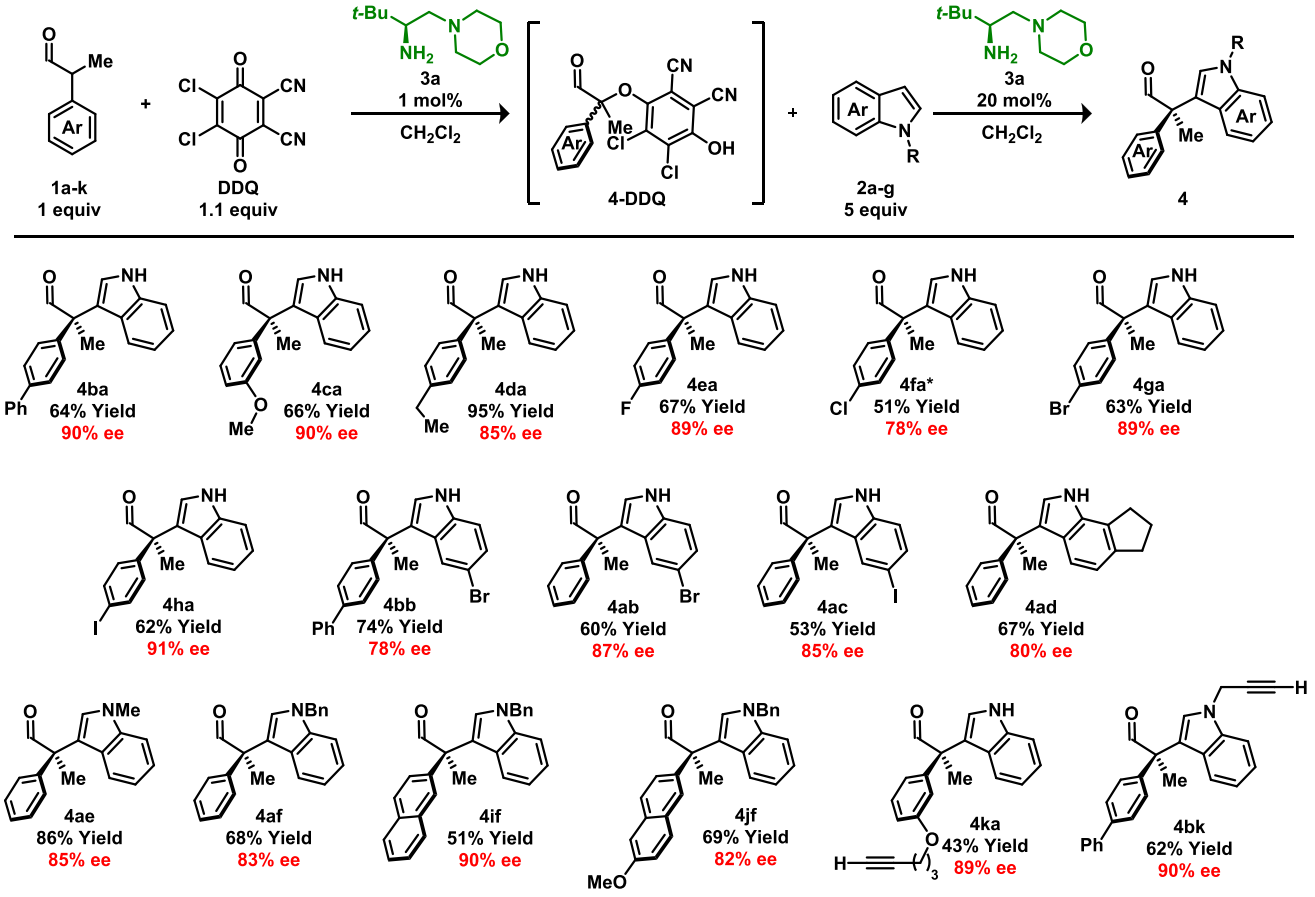

[a]Absolute configuration was determined using single-crystal X-ray crystallography of **4bb** and assigned in analogy. * = Starting from the **4-DDQ**.

hydroquinone, which contributes to a 2.4 kcal/mol energy difference of the transition states of two equilibrating reactive imine species and renders the substitution by the zwitterionic species the preferred pathway. The uncatalyzed background pathway is the least competitive due to the necessity of an endergonic hydrolysis.[40]

The calculated S_N2 mechanism suggests that the reactive center, **4e-DDQ**, is condensed with the aminocatalyst **3a**. As such, kinetic experiments were performed to determine an order in the aminocatalyst (Figure 4, top). Since the catalyst is required to generate the DDQ adduct, amendments to the previously applied conditions were made to ensure appropriate interpretations (see Supporting Information). The DDQ adduct was generated *in situ* using 1 mol % aminocatalyst. Upon complete conversion to the adduct, supplementary aminocatalyst (1−10 mol %) was added followed by 40 equiv of indole (Figure 4, top). A proportional initial rate enhancement progressed with increased concentrations of aminocatalyst indicating a first-order dependence, consistent with the computed rate-determining step. The resulting *y*-intercept is consistent with an uncatalyzed background reaction as a minor reaction pathway (Figure 4, bottom).

Origin of Stereoselectivity in the S_N2 Reaction. Based on the computational studies, the oxidation of the enamine intermediate is unselective and provides both enantiomers in near equal quantities. As a consequence, the stereodetermining step would occur postoxidation and during the course of the bimolecular indole substitution reaction. To directly probe the hypothesis, the intermediate was formed using an achiral catalyst, isolated as a racemate, and subjected to two distinct, stereodetermining conditions shown in eq 2 and eq 3. When

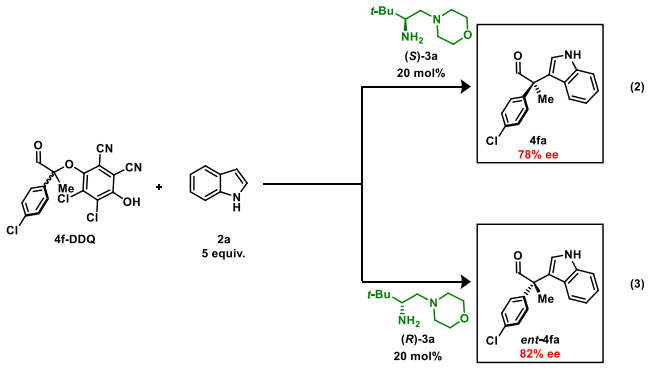

applying aminocatalyst (*S*)-**3a**, the product **4fa** was formed with 78% ee (eq 2). However, application of the aminocatalyst (*R*)-**3a** led to a complete shift in the favored enantiomer resulting in 82% ee of *ent*-**4fa** (eq 3). Furthermore, omission of aminocatalyst resulted in the racemic formation of the indole coupled product. These studies succinctly exhibit the enantioselectivity as a salient feature of the aminocatalyst.

Upon condensation of the primary amine catalyst with the DDQ adduct, intramolecular interactions may promote the

https://doi.org/10.1021/jacs.1c02193
J. Am. Chem. Soc. 2021, 143, 7509−7520

substitution of one diastereomer over another. Two lowest-energy diastereomeric transition states calculated for the substitution step are presented in Figure 5A. Aside from the stacking interaction existing in both diastereomeric transition states, the diastereomeric transition state whose leaving hydroquinone is located on the top of the imine plane benefits from a 1.58 Å hydrogen bonding with the morpholine moiety (TS-major), while the other has a much weaker C−H···N interaction of 2.21 Å with the incoming indole placed at the top (TS-minor). This critical interaction again plays the decisive role by introducing the chirality of the aminocatalyst to the substitution process, leading to satisfying enantioselectivity. Accordingly, a 1.5 kcal/mol difference in enthalpy is obtained between the two diastereomeric transition states. Figure 5A shows both the $\Delta\Delta H^{\ddagger}$ and $\Delta\Delta G^{\ddagger}$ values, since we found that the E and H at various levels always give a preference for TS-major, while the ΔG values are near zero and favor the major or the minor TS at different computational levels. The kinetic preference does agree with the observed enantioselectivity; however, complete consumption of starting material and yields greater than 50% from a racemate rule out a kinetic resolution regime.[8,19,26,27] These key attributes imply a stereomutative transformation prior to indole substitution. More specifically, enantiomeric excess as a function of time appears marginally insensitive to conversion dependence and most closely resembles a DYKAT (dynamic kinetic asymmetric transformation) type 1 scenario, as shown in Figure 5B.[26]

One baffling aspect in this process is that since the indole substitution step is rate-determining and highly exergonic, the stereomutative transformation could not be feasible unless it is much faster and highly reversible, requiring a much better nucleophile than indole in the reaction system. We investigated the possibility of epimerization of the stereocenter driven by the self-substitution of hydroquinone.[8] DFT calculations were performed to test this hypothesis (Figure 6A). Indeed, an *R*-zwitterionic intermediate is found to be in a fast equilibrium with its *S*-diastereomer. The indistinguishable energies of these diastereomers predict that they will be a 1:1 mixture at equilibrium; one of these can then undergo the indole substitution at a faster rate, resulting in the major observed enantiomer. A transition state of self-substitution is located with a 20.3 kcal/mol energy barrier and should then be faster than substitution with indole (∼30 kcal/mol, Figure 3). In this interconversion process, the morpholine moiety on the aminocatalyst subtly directs the incoming hydroquinone: the basic tertiary amine deprotonates the hydroquinone and forms a hydrogen bond during the self-substitution. At the same time, the negative charge is prone to concentrate on the attacking oxygen atom of hydroquinone. The hydroquinone hence exhibits an anionic property in the transition state, making it a better nucleophile relative to indole. The unexpected S_N2-DKR nicely explains the behavior of enantiomeric excess and conversion rate, *though violating the common intuition that Walden inversion occurs on a definitive stereocenter during S_N2. In fact, this process is an exemplar model of the Curtin−Hammett principle.*

Trifunctional Role of the Aminocatalyst. To indirectly probe the occurrence of the stereomutative transformation prior to the rate-determining indole substitution, the enantiomeric excess was evaluated as a function of aminocatalyst loading. As shown in Figure 6B, the observed correlation affirms aminocatalyst involvement in the preceding interconversion step of the reaction mechanism. A near racemic mixture of product at low catalyst concentrations is consistent with an unselective oxidation and a diminished rate of interconversion prior to indole substitution.

Additional studies were performed to confirm the vital role of the tertiary amine moiety. The protonation of the morpholine moiety on the aminocatalyst plays multiple roles throughout the substitution: that is, it promotes the hydroquinone-mediated stereomutative interconversion, facilitating indole substitution by stabilizing the transition state and effectuating the stereoinduction from the chiral aminocatalyst. To further expose the function of this molecular fragment, we have conducted an intrinsic reaction coordinate (IRC) calculation for the substitution process (Figure 6C). Bond lengths of the cleaving C−O bond and the critical hydrogen bond are recorded at each point along the IRC pathway. Starting with the plots that represent the primary structures of the reaction at the left top, the hydrogen bond length changes from ∼2.15 Å to 2.00 Å as the C−O bond cleaves, suggesting that this hydrogen bonding initiates the "abstraction" of the C−O bond by strengthening the attractive force of O···H interaction. Subsequently, a remarkable linear correlation appears as the C−O bond is cleaving, ranging from 1.6 to 3.1 Å, clearly corresponding to the stabilization effect of the hydrogen bond. The transition state is located at the late stage of this region. After the leaving group has been completely substituted by the nucleophile, the hydrogen bonding is fortified to a higher degree, neutralizing the negative charge on the leaving group.

From the IRC in Figure 6C, it was found that the N−H of the protonated morpholino moiety in the catalyst clearly plays an important role. To experimentally investigate this, a catalyst without the amine moiety was prepared. The amine-bearing morpholine group in catalyst **3a** was substituted for the isostere cyclohexyl for catalyst **3b** (eq 4 and eq 5). As a result,

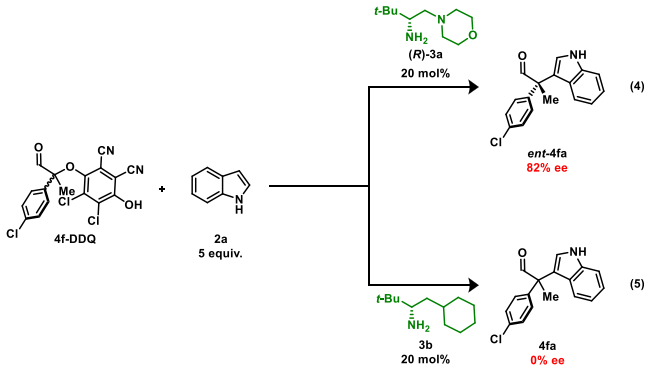

differences in reactivity can be ascribed to the lack of H-bonding interactions. Remarkably, a racemic mixture of products was obtained when this isostere was used, despite the aminocatalyst bearing an identical stereocenter.[41] This emphasizes the pivotal role of the H-bonding interactions deduced in the IRC to achieve high enantioselectivity.

In placing these empirical studies in the greater context of the density functional theory (DFT) calculations, these results affirm a Curtin−Hammett regime initiated by the tertiary amine moiety of the catalyst. Notably, the dynamic self-substitution pathway describing the racemization of the DDQ adduct is reminiscent of the Walden cycle.[1−4,6] In analogy, both enantiomers of the reactive DDQ adduct are accessible by consecutive S_N2 reactions as depicted in Figure 7A. An enantiomer of the DDQ adduct is condensed with the chiral

https://doi.org/10.1021/jacs.1c02193
J. Am. Chem. Soc. 2021, 143, 7509−7520

aminocatalyst to form a transient diastereomer. The resulting diastereomer is in equilibrium with its epimer traversed through the self-substitution and, finally, hydrolyzed to provide access to the antipodal enantiomer. Departure from the racemization event ensues upon the rate-determining substitution with indole. As a consequence of the differences in enthalpy between TS-major and TS-minor, the dynamic Walden cycle allows for the indole substitution to primarily funnel through one diastereomer, rendering the S_N2 stereoselective. *Together these two processes combine to establish the asymmetric S_N2 dynamic kinetic resolution reaction.* Remarkably, a single aminocatalyst facilitates the conversion of racemic starting material to enantioenriched product through the use of three distinct catalytic cycles, as depicted in Figure 7B.

Mechanistically Guided Methodology. Based on the novel mechanistic principles identified in the S_N2-DKR pathway, the methodology for the enantioselective formation of quaternary carbon stereocenters was refined (Scheme 4). We have identified that the oxidation process can proceed with only 1 mol % aminocatalyst leading to racemic **4-DDQ**. Since aminocatalysts could be deactivated under oxidizing conditions, only 1 mol % of catalyst was employed to oxidize the aldehyde to the DDQ adduct. Upon full conversion to the intermediate, 20 mol % of aminocatalyst was added in conjunction with the indole nucleophile. This adaptation maximized the aminocatalyst concentration for the S_N2-DKR and allows for the enantioselective addition of indoles to electron-neutral and -deficient α-branched aldehydes with a variety of indoles. Notably, these aldehydes were incompatible with previously established methodologies. Aldehydes bearing *para*-substituted halogens are amenable to this protocol, providing complementary and facile access to increased complexity via the aldehyde or aryl halide synthon. Furthermore, *N*-alkylated indoles cleanly furnished the desired products, indicating minimal influence of the N−H moiety. Finally, the methodology was applied to derivatize a pharmaceutical (naproxen) and translated to compounds suitable for bioconjugation via click chemistry. Generally, moderate to high yields were obtained with high enantioselectivity to form a quaternary carbon stereocenter through this unusual S_N2-DKR process at a tertiary carbon center.

CONCLUSION

By integrating DFT, kinetic, and empirical studies, we have uncovered an atypical pathway for the catalytic, stereoselective formation of quaternary carbon stereocenters. This pathway consists of three elementary steps: (1) oxidation of the enamine species, (2) racemization, and (3) substitution. Peculiar aspects include an S_N2-DKR event resembling a dynamic Walden cycle (epimerization via S_N2 reaction) terminated by a rate-determining S_N2 at a tetrasubstituted tertiary center. Through a Curtin−Hammett regime, the stereospecific S_N2 also becomes stereoselective, effectively distinguishing between two transient diastereomers. Notably computational and experimental studies have shown that the aminocatalyst bearing a primary amine for condensation and a tertiary amine moiety for hydrogen bonding is essential in each of the three elementary steps of the reaction. These studies were instructive in refining the protocol to develop a more general methodology. Moreover, our investigations establish that stereomutative processes can occur through an S_N2 mechanism and permit stereoselective reactions through a stereospecific substitution. We anticipate these results to rekindle interest in the S_N2 mechanism as a synthetic tool for stereoselective reactions.[42]

ASSOCIATED CONTENT

Supporting Information

The Supporting Information is available free of charge at https://pubs.acs.org/doi/10.1021/jacs.1c02193.

Experimental procedures, characterization data, NMR spectra, UPCC spectra, theoretical calculations (PDF)

Accession Codes

CCDC 2034477 contains the supplementary crystallographic data for this paper. These data can be obtained free of charge via www.ccdc.cam.ac.uk/data_request/cif, or by emailing data_request@ccdc.cam.ac.uk, or by contacting The Cambridge Crystallographic Data Centre, 12 Union Road, Cambridge CB2 1EZ, UK; fax: +44 1223 336033.

AUTHOR INFORMATION

Corresponding Authors

Karl Anker Jørgensen − *Department of Chemistry, Aarhus University, DK-8000 Aarhus C, Denmark;* orcid.org/0000-0002-3482-6236; Email: kaj@chem.au.dk

K. N. Houk − *Department of Chemistry and Biochemistry, University of California, Los Angeles, California 90095, United States;* orcid.org/0000-0002-8387-5261; Email: houk@chem.ucla.edu

Authors

Nomaan M. Rezayee − *Department of Chemistry, Aarhus University, DK-8000 Aarhus C, Denmark;* orcid.org/0000-0002-9622-6324

Valdemar J. Enemærke − *Department of Chemistry, Aarhus University, DK-8000 Aarhus C, Denmark*

Sif T. Linde − *Department of Chemistry, Aarhus University, DK-8000 Aarhus C, Denmark*

Johannes N. Lamhauge − *Department of Chemistry, Aarhus University, DK-8000 Aarhus C, Denmark*

Gabriel J. Reyes-Rodríguez − *Department of Chemistry, Aarhus University, DK-8000 Aarhus C, Denmark;* orcid.org/0000-0002-0566-0820

Chenxi Lu − *Department of Chemistry and Biochemistry, University of California, Los Angeles, California 90095, United States*

Complete contact information is available at: https://pubs.acs.org/10.1021/jacs.1c02193

Notes

The authors declare no competing financial interest.

ACKNOWLEDGMENTS

K.A.J. thanks Villum Investigator grant (no. 25867), the Carlsberg Foundation "Semper Ardens", and Aarhus University. We also thank Mathias Kirk Thøgersen for elucidation of the X-ray structure of **4bb**. Access to instruments at the Danish Center for Ultrahigh-Field NMR Spectroscopy funded by the Danish Ministry of Higher Education and Science (AU-2010-612-181) is acknowledged. Computations were performed on the Hoffman2 cluster at UCLA and the Extreme Science and Engineering Discovery Environment (XSEDE), which is supported by the National Science Foundation (OCI-1053575). We are grateful for financial support of the UCLA

work from the National Science Foundation (CHE-1764328 to K.N.H.).

REFERENCES

(1) Ingold, C. K. *Structure and Mechanisms in Organic Chemistry*; Cornell University Press: Ithaca, NY, 1953.
(2) Walden, P. Ueber die Gegenseitige Umwandlung Optischer Antipoden. *Ber. Dtsch. Chem. Ges.* **1896**, *29*, 133−138.
(3) Kenyon, J.; Phillips, H. Some Recent Developments in the Study of the Walden Inversion. *Trans. Faraday Soc.* **1930**, *26*, 451−458.
(4) Hughes, E. D.; Juliusburger, F.; Masterman, S.; Topley, B.; Weiss, J. 362. Aliphatic Substitution and the Walden Inversion. Part I. *J. Chem. Soc.* **1935**, 1525−1529.
(5) Cowdrey, W. A.; Hughes, E. D.; Ingold, C. K.; Masterman, S.; Scott, A. D. 257. Reaction Kinetics and the Walden Inversion. Part VI. Relation of Steric Orientation to Mechanism in Substitutions Involving Halogen Atoms and Simple or Substituted Hydroxyl Groups. *J. Chem. Soc.* **1937**, 1252−1271.
(6) Buchanan, J. G.; Diggle, R. A.; Ruggiero, G. D.; Williams, I. H. The Walden Cycle Revisited: a Computational Study of Competitive Ring Closure to α- and β-Lactones. *Chem. Commun.* **2006**, 1106−1108.
(7) Ansyln, E. V. D., Dougherty, D. A. *Modern Physical Organic Chemistry*; University Science Books: Herndon, VA, 2005.
(8) Bartoszewicz, A.; Matier, C. D.; Fu, G. C. Enantioconvergent Alkylations of Amines by Alkyl Electrophiles: Copper-Catalyzed Nucleophilic Substitutions of Racemic α-Halolactams by Indoles. *J. Am. Chem. Soc.* **2019**, *141*, 14864−14869.
(9) Kubo, A.; Takahashi, M.; Kubota, H.; Nunami, K. Dynamic Kinetic Resolution Utilizing a Chiral Auxiliary by Stereoselective S_N2 Alkylation with Malonic Ester Enolate. *Tetrahedron Lett.* **1995**, *36*, 6251−6252.
(10) Kubota, H.; Kubo, A.; Takahashi, M.; Shimizu, R.; Da-te, T.; Okamura, K.; Nunami, K.-i. Stereospecific Amination by Dynamic Kinetic Resolution Utilizing 2-Oxoimidazolidine-4-carboxylate as a Novel Chiral Auxiliary. *J. Org. Chem.* **1995**, *60*, 6776−6784.
(11) Seebach, D.; Sting, A. R.; Hoffmann, M. Self-Regeneration of Stereocenters (SRS)—Applications, Limitations, and Abandonment of a Synthetic Principle. *Angew. Chem., Int. Ed. Engl.* **1996**, *35*, 2708−2748.
(12) Lanke, V.; Marek, I. Nucleophilic Substitution at Quaternary Carbon Stereocenters. *J. Am. Chem. Soc.* **2020**, *142*, 5543−5548.
(13) Edwards, O. E.; Grieco, C. S_N2 Displacement at Tertiary Carbon. *Can. J. Chem.* **1974**, *52*, 3561−3562.
(14) Shibatomi, K.; Soga, Y.; Narayama, A.; Fujisawa, I.; Iwasa, S. Highly Enantioselective Chlorination of β-Keto Esters and Subsequent S_N2 Displacement of Tertiary Chlorides: A Flexible Method for the Construction of Quaternary Stereogenic Centers. *J. Am. Chem. Soc.* **2012**, *134*, 9836−9839.
(15) Mukaiyama, T.; Shintou, T.; Fukumoto, K. A Convenient Method for the Preparation of Inverted tert-Alkyl Carboxylates from Chiral tert-Alcohols by a New Type of Oxidation−Reduction Condensation Using 2,6-Dimethyl-1,4-benzoquinone. *J. Am. Chem. Soc.* **2003**, *125*, 10538−10539.
(16) Mascal, M.; Hafezi, N.; Toney, M. D. 1,4,7-Trimethyloxatriquinane: S_N2 Reaction at Tertiary Carbon. *J. Am. Chem. Soc.* **2010**, *132*, 10662−10664.
(17) Pronin, S. V.; Reiher, C. A.; Shenvi, R. A. Stereoinversion of Tertiary Alcohols to Tertiary-alkyl Isonitriles and Amines. *Nature* **2013**, *501*, 195−199.
(18) Blom, J.; Reyes-Rodríguez, G. J.; Tobiesen, H. N.; Lamhauge, J. N.; Iversen, M. V.; Barløse, C. L.; Hammer, N.; Rusbjerg, M.; Jørgensen, K. A. Umpolung Strategy for α-Functionalization of Aldehydes for the Addition of Thiols and other Nucleophiles. *Angew. Chem., Int. Ed.* **2019**, *58*, 17856−17862.
(19) Vedejs, E.; Jure, M. Efficiency in Nonenzymatic Kinetic Resolution. *Angew. Chem., Int. Ed.* **2005**, *44*, 3974−4001.
(20) Zhang, X.; Ren, J.; Tan, S. M.; Tan, D.; Lee, R.; Tan, C.-H. An Enantioconvergent Halogenophilic Nucleophilic Substitution (S_N2X) Reaction. *Science* **2019**, *363*, 400−404.
(21) Yang, Y.; Cho, I.; Qi, X.; Liu, P.; Arnold, F. H. An Enzymatic Platform for the Asymmetric Amination of Primary, Secondary and Tertiary C(sp3)−H bonds. *Nat. Chem.* **2019**, *11*, 987−993.
(22) Ren, J.; Ban, X.; Zhang, X.; Tan, S. M.; Lee, R.; Tan, C. H. Kinetic and Dynamic Kinetic Resolution of Racemic Tertiary Bromides by Pentanidium-Catalyzed Phase-Transfer Azidation. *Angew. Chem., Int. Ed.* **2020**, *59*, 9055−9058.
(23) Guo, W.; Luo, Y.; Sung, H. H.; Williams, I. D.; Li, P.; Sun, J. Chiral Phosphoric Acid Catalyzed Enantioselective Synthesis of α-Tertiary Amino Ketones from Sulfonium Ylides. *J. Am. Chem. Soc.* **2020**, *142*, 14384−14390.
(24) Yang, C.-J.; Zhang, C.; Gu, Q.-S.; Fang, J.-H.; Su, X.-L.; Ye, L.; Sun, Y.; Tian, Y.; Li, Z.-L.; Liu, X.-Y. Cu-catalysed Intramolecular Radical Enantioconvergent Tertiary β-C(sp3)−H Amination of Racemic Ketones. *Nat. Catal.* **2020**, *3*, 539−546.
(25) Wang, Z.; Yang, Z.-P.; Fu, G. C. Quaternary Stereocentres via Catalytic Enantioconvergent Nucleophilic Substitution Reactions of Tertiary Alkyl Halides. *Nat. Chem.* **2021**, *13*, 236.
(26) Steinreiber, J.; Faber, K.; Griengl, H. De-racemization of Enantiomers versus De-epimerization of Diastereomers—Classification of Dynamic Kinetic Asymmetric Transformations (DYKAT). *Chem. - Eur. J.* **2008**, *14*, 8060−8072.
(27) Mohr, J. T.; Moore, J. T.; Stoltz, B. M. Enantioconvergent Catalysis. *Beilstein J. Org. Chem.* **2016**, *12*, 2038−2045.
(28) Quasdorf, K. W.; Overman, L. E. Catalytic Enantioselective Synthesis of Quaternary Carbon Stereocentres. *Nature* **2014**, *516*, 181−191.
(29) Liu, Y.; Han, S.-J.; Liu, W.-B.; Stoltz, B. M. Catalytic Enantioselective Construction of Quaternary Stereocenters: Assembly of Key Building Blocks for the Synthesis of Biologically Active Molecules. *Acc. Chem. Res.* **2015**, *48*, 740−751.
(30) Leth, L. A.; Næsborg, L.; Reyes-Rodríguez, G. J.; Tobiesen, H. N.; Iversen, M. V.; Jørgensen, K. A. Enantioselective Oxidative Coupling of Carboxylic Acids to α-Branched Aldehydes. *J. Am. Chem. Soc.* **2018**, *140*, 12687−12690.
(31) Rezayee, N. M.; Lauridsen, V. H.; Næsborg, L.; Nguyen, T. V. Q.; Tobiesen, H. N.; Jørgensen, K. A. Oxidative Organocatalysed Enantioselective Coupling of Indoles with Aldehydes that Forms Quaternary Carbon Stereocentres. *Chem. Sci.* **2019**, *10*, 3586−3591.
(32) Tobiesen, H. N.; Leth, L. A.; Iversen, M. V.; Næsborg, L.; Bertelsen, S.; Jørgensen, K. A. Stereoselective Oxidative Bioconjugation of Amino Acids and Oligopeptides to Aldehydes. *Angew. Chem., Int. Ed.* **2020**, *59*, 18490−18494.
(33) Baran, P. S.; Richter, J. M. Direct Coupling of Indoles with Carbonyl Compounds: Short, Enantioselective, Gram-Scale Synthetic Entry into the Hapalindole and Fischerindole Alkaloid Families. *J. Am. Chem. Soc.* **2004**, *126*, 7450−7451.
(34) Beeson, T. D.; Mastracchio, A.; Hong, J.-B.; Ashton, K.; MacMillan, D. W. C. Enantioselective Organocatalysis Using SOMO Activation. *Science* **2007**, *316*, 582−585.
(35) Murphy, J. J.; Bastida, D.; Paria, S.; Fagnoni, M.; Melchiorre, P. Asymmetric Catalytic Formation of Quaternary Carbons by Iminium Ion Trapping of Radicals. *Nature* **2016**, *532*, 218−222.
(36) Wendlandt, A. E.; Vangal, P.; Jacobsen, E. N. Quaternary Stereocentres via an Enantioconvergent Catalytic S_N1 Reaction. *Nature* **2018**, *556*, 447−451.
(37) Guo, X.; Mayr, H. Manifestation of Polar Reaction Pathways of 2,3-Dichloro-5,6-dicyano-p-benzoquinone. *J. Am. Chem. Soc.* **2013**, *135*, 12377−12387.
(38) Shevchenko, G. A.; Oppelaar, B.; List, B. An Unexpected α-Oxidation of Cyclic Ketones with 1,4-Benzoquinone by Enol Catalysis. *Angew. Chem., Int. Ed.* **2018**, *57*, 10756−10759.
(39) Phan, T. B.; Nolte, C.; Kobayashi, S.; Ofial, A. R.; Mayr, H. Can One Predict Changes from S_N1 to S_N2 Mechanisms? *J. Am. Chem. Soc.* **2009**, *131*, 11392−11401.

https://doi.org/10.1021/jacs.1c02193
J. Am. Chem. Soc. 2021, 143, 7509−7520

(40) Leung, B. O.; Reid, D. L.; Armstrong, D. A.; Rauk, A. Entropies in Solution from Entropies in the Gas Phase. *J. Phys. Chem. A* **2004**, *108*, 2720−2725.
(41) Wang, Y.; Zhou, H.; Yang, K.; You, C.; Zhang, L.; Luo, S. Steric Effect of Protonated Tertiary Amine in Primary-Tertiary Diamine Catalysis: A Double-Layered Sterimol Model. *Org. Lett.* **2019**, *21*, 407−411.
(42) Xie, J.; Hase, W. L. Rethinking the S_N2 Reaction. *Science* **2016**, *352*, 32−33.

https://doi.org/10.1021/jacs.1c02193
J. Am. Chem. Soc. 2021, 143, 7509−7520